Mesoporous Thin Films of "Molecular Squares" as Sensors for Volatile Organic Compounds

Melinda H. Keefe,† Robert V. Slone, Joseph T. Hupp,*,† Kenneth F. Czaplewski,‡ Randall Q. Snurr,‡ and Charlotte L. Stern

Departments of Chemistry and Chemical Engineering, Northwestern University, 2145 Sheridan Road, Evanston, Illinois 60208-3114

Received September 20, 1999. In Final Form: December 31, 1999

Mesoporous thin films of rhenium-based "molecular squares", $[Re(CO)_3Cl(L)]_4$ (L = pyrazine, 4,4′-bipyridine), have been utilized as sensors for volatile organic compounds (VOCs). The sensing was conducted using a quartz crystal microbalance with the target compounds present in the gas phase at concentrations ranging from 0.05 to 1 mM. Quartz crystal microbalance studies with these materials allowed for distinction between the following VOCs: (1) small aromatic versus aliphatic molecules of almost identical size and volatility and (2) an array of benzene molecules derivatized with electron donating/withdrawing substituents. The experiments suggest that the mesoporous host materials interact with VOC guest molecules through both van der Waals and weak charge-transfer interactions. In addition, size selectivity is shown by exposure of the molecular squares to cyclic ethers of differing size.

Introduction

There has been tremendous recent interest in the assembly and self-assembly of transition-metal-based "molecular squares"[1−8] and related ligand-bridged metallacycles (rectangles,[9] triangles,[10] hexagons,[11] etc.). A compelling research driver, in addition to molecular aesthetics, has been the possibility of using the cavity-containing metallacycles as nanoscale hosts in chemical recognition and sensing processes. Extant proof-of-concept investigations of the relevant host/guest interactions have largely emphasized solution-phase NMR detection,[1a−c,12] although in a few cases solution-phase electrochemical[12−16] or luminescence detection[3,4,6,12,15] has been utilized. An alternative heterogeneous approach, based on guest recognition and binding by high-porosity molecular *materials*, would prove complementary to homogeneous approaches—and, in some cases, highly advantageous. For example, in many sensing environments an inherently heterogeneous approach might prove more versatile in terms of potential analyte composition, more practical in terms of actual device implementation, and more sensitive than some homogeneous approaches (most notably, conventional NMR approaches, which can be difficult to use when sample concentrations are less than a few tenths of a millimole per liter).

We report here on the use of porous molecular materials as thin-film arrays of host or molecular-recognition sites, deposited on the surface of a quartz crystal microbalance, for selected volatile organic chemical (VOC) guest species. The building blocks for the films were the tetrametallic pyrazine- and 4,4′-bipyridine-bridged squares, **1** and **2,** as well as related corner assemblies, **3** and **4**. We also report on the single-crystal structure of one of the molecular materials, **4**.

* To whom correspondence should be addressed. Fax: (847) 491-7713. E-mail: jthupp@chem.nwu.edu.

† Department of Chemistry.

‡ Department of Chemical Engineering.

(1) (a) Fujita, M.; Yakazi, J.; Ogura, K. *J. Am. Chem. Soc.* **1990**, *112*, 5645. (b) Fujita, M.; Nagao, S.; Iida, M.; Ogata, K. *J. Am. Chem. Soc.* **1993**, *115*, 1574. (c) Fujita, M.; Yakazi, J.; Ogura, K. *Tetrahedron Lett.* **1991**, *32*, 5589. (d) Fujita, M.; Yazaki, J.; Ogura, K. *Chem. Lett.* **1991**, 1031.

(2) (a) Stang, P. J.; Cao, D. H. *J. Am. Chem. Soc.* **1994**, *116*, 4981. (b) Stang, P. J.; Chen, K.; Arif, A. M. *J. Am. Chem. Soc.* **1995**, *117*, 8973. (c) Stang, P. J.; Cao, D. H.; Saito, S.; Arif, A. M. *J. Am. Chem. Soc.* **1995**, *117*, 6273. (d) Stang, P. J.; Olenyuk, B.; Fan, J.; Arif, A. M. *Organometallics* **1996**, *15*, 904. (e) Stang, P. J.; Olenyuk, B. *Angew. Chem., Int. Ed. Engl.* **1996**, *35*, 732. (f) Stang, P. J.; Persky, N. E. *J. Chem. Soc., Chem. Commun.* **1997**, 77. (g) Whiteford, J. A.; Lu, C. V.; Stang, P. J. *J. Am. Chem. Soc.* **1997**, *119*, 2524. (h) Stang, P. J.; Cao, D. H.; Chen, K.; Gray, G. M.; Muddiman, D. C.; Smith, R. D. *J. Am. Chem. Soc.* **1997**, *119*, 5163. (i) Stang, P. J.; Fan, J.; Olenyuk, B. *J. Chem. Soc., Chem. Commun.* **1997**, 1453.

(3) Slone, R. V.; Yoon, D. I.; Calhoun, R. M.; Hupp, J. T. *J. Am. Chem. Soc.* **1995**, *117*, 11813.

(4) Slone, R. V.; Hupp, J. T.; Stern, C. L.; Albrecht-Schmitt, T. E. *Inorg. Chem.* **1996**, *35*, 4096.

(5) Slone, R. V.; Hupp, J. T. *Inorg. Chem.* **1997**, *36*, 5422.

(6) Slone, R. V.; Benkstein, K. D.; Bélanger, S.; Hupp, J. T.; Guzei, I. A.; Rheingold, A. L. *Coord. Chem. Rev.* **1998**, *171*, 221.

(7) (a) Leung, W.-H.; Cheng, J. Y. K.; Hun, T. S. M.; Che, C.-M.; Wong, W. T.; Cheung, K.-K. *Organometallics* **1996**, *15*, 1497. (b) Kalb, W. C.; Demidowicz, Z.; Speckmann, D. M.; Knobler, C.; Teller, R. G.; Hawthorne, M. F. *Inorg. Chem.* **1982**, *21*, 4027. (c) Stricklen, P. M.; Volcko, E. J.; Verkade, J. G. *Inorg. Chem.* **1983**, *22*, 2494.

(8) For recent reviews see ref 6 and the following: (a) Fujita, M.; Ogura, G. *Bull. Chem. Soc. Jpn.* **1996**, *69*, 1471. (b) Stang, P. J.; Olenyuk, B. *Acc. Chem. Soc.* **1997**, *30*, 502. (c) Cao, D. H.; Chen, K. C.; Fan, J.; Manna, J.; Olenyuk, B.; Whiteford, J. A.; Stang, P. J. *Pure Appl. Chem.* **1997**, *69*, 1979. (d) Olenyuk, B.; Fechtenkotter, A.; Stang, P. J. *J. Chem. Soc., Dalton Trans.* **1998**, *11*, 1707. (e) Jones, C. J. *Chem. Soc. Rev.* **1998**, *27*, 289.

(9) (a) Benkstein, K. D.; Hupp, J. T.; Stern, C. L. *J. Am. Chem. Soc.* **1998**, *120*, 12982. (b) Benkstein, K. D.; Hupp, J. T.; Stern, C. L. *Inorg. Chem.* **1998**, *37*, 5404.

(10) (a) Fujita, M.; Sasaki, O.; Mitsuhashi, T.; Fujita, T.; Yazaki, J.; Yamaguchi, K.; Ogura, K. *J. Chem. Soc., Chem. Commun.* **1996**, 1535. (b) Schnebeck, R.-D.; Randaccio, L.; Zangrando, E.; Lippert, B. *Angew. Chem., Int. Ed. Engl.* **1998**, *37*, 119.

(11) (a) Lai, S.-W.; Cheung, K.-K.; Chan M. C.-W.; Che, C.-M. *Angew. Chem., Int. Ed. Engl.* **1998**, *37*, 182. (b) Stang, P. J.; Persky, N. E.; Manna, J. *J. Am. Chem. Soc.* **1997**, *119*, 4777. (c) Hall, J. R.; Loeb, S. J.; Scimizu, G. K. H.; Yap, G. P. A. *Angew. Chem., Int. Ed. Engl.* **1998**, *37*, 121.

(12) Beer, P. D.; Szemes, F.; Balzani, V.; Sala, C. M.; Drew, M. G. B.; Dent, S. W.; Maistri, M. *J. Am. Chem. Soc.* **1997**, *119*, 11864.

(13) Bélanger, S.; Hupp, J. T.; Slone, R. V.; Watson, D. F.; Carrell, T. *J. Am. Chem. Soc.* **1999**, *121*, 557.

(14) Bélanger, S.; Hupp, J. T. *Angew. Chem., Int. Ed. Engl.* **1999**, *38*, 2222.

(15) Beer, P. D. *Chem. Commun.* **1996**, 689.

(16) Bélanger, S.; Anderson, B. C.; Hupp, J. T. *Proc. Electrochem. Soc.* **1998**, *98−26*, 208.

10.1021/la991252k CCC: $19.00
Published on Web 03/04/2000

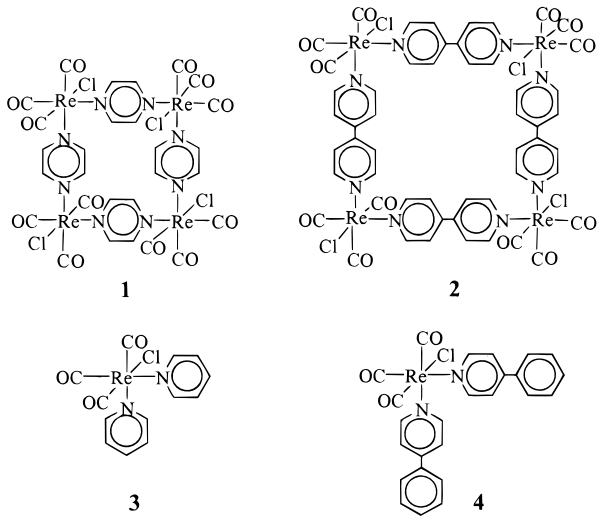

1 **2**

3 **4**

Compounds **1** and **2** were deemed particularly attractive as VOC-responsive materials because they (a) feature cavity sizes that are comparable to target guest sizes (minimum cavity diameters of ca. 5 Å (**1**) and 9 Å (**2**)), (b) are neutral and therefore lack cavity-blocking counterions which would necessarily accompany charged host assemblies,[17] (c) display high solubility in polar organic solvents, thereby permitting film preparation via simple evaporative casting, but (d) exhibit complete insolubility in water, thus permitting the assembly of films which are durable in aqueous environments. In addition, as shown in Figures 1 and 2, the compounds form infinite, one-dimensional, zeolite-like channels in the crystalline solid state.[4,13] Thus, the molecular cavities are aligned appropriately to accommodate guest transport via simple unidirectional diffusion. The X-ray structures also indicate free volumes of 48 and 27% for **1** and **2**, respectively.[18] (The smaller square has the larger void volume because of pockets present in the packing of the solid-state structure; see Figure 1.) Shown for comparison in Figure 3 is a space-filled representation of the packing structure of a single crystal of **4**. Note the dense packing and absence of channels. The packing structure for **3** similarly lacks channels.[19] The free volumes for **3** and **4** are 2.5 and 7%, respectively. For **1** and **2**, further evidence for thin-film mesoporosity and guest-size-dependent interior accessibility implied by the crystal structures is shown by recently reported electrochemical molecular sieving experiments.[13,16]

Given the apparently good film accessibility and mesoporosity, we reasoned that VOC guest uptake could be readily monitored in real time via quartz crystal microgravimetry (QCM). This technique and related surface acoustic wave (SAW) techniques rely upon the sensitivity of the oscillation frequency of the piezoelectric platform (quartz) to changes in device mass—where the required mass changes come from guest uptake by a coating of host material. It should be noted that several host molecule functionalized piezoelectric sensor assemblies based on monolayer coatings have been reported previously.[20] Because of the inherently small absolute guest uptake capacity of monolayer systems, however, their applicability is limited either to host/guest pairs displaying exceptionally large association constants or to guests present at comparatively high vapor pressures. The constraints associated with monolayer systems translate into higher detection limits and smaller dynamic ranges than achievable with multilayer host systems. Perhaps functionally, if not structurally, more closely related to our studies are recent studies by Finklea and co-workers of a clathrate-forming nickel(II) compound as a multilayer sensor coating, where the targets of the sensor were several common volatile organic compounds.[21] Also pertinent is a series of studies of multilayers of organic macrocycles (e.g., cyclodextrins and paracyclophanes) as selective receptor materials in piezoelectric-based devices.[22]

As outlined below, we find that QCM-type sensors featuring thin films of **1** and **2** respond reversibly to selected VOCs, where modest selectivity is achievable based both on host/guest cavity size matching and on host/guest chemical complementarity. In contrast, thin films of **3** and **4** were found to be unresponsive to VOC vapors.

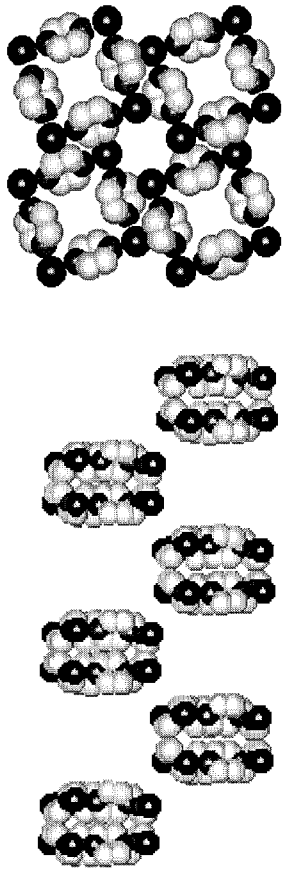

Figure 1. Top: Space-filled representation of the single-crystal X-ray structure of **1** along the *c* crystallographic axis,[4] showing the presence of unidirectional open-ended channels. Bottom: Space-filled representation of the structure in the *bc* plane, showing the offset between the molecular squares on adjacent layers. For clarity, we have omitted the one chloro and three carbonyl ligands surrounding each metal atom (corner atom). The solvent molecules (omitted for clarity) are located in the pockets between the tetranuclear assemblies.

(17) Counterions present with charged host assemblies could, of course, lie either within or outside of the host cavity.

(18) A second polymorph of **2** has been reported with the molecules flat rather than puckered. Its void volume is 49% of the total volume.[13]

(19) Bélanger, S.; Hupp, J. T.; Stern, C. L. *Acta Crystallogr.* **1998**, *C54*, 1596.

(20) (a) Dickert, F. L.; Bruckdorfer, Th.; Feigl, H.; Haunschild, A.; Kuschow, V.; Obermeier, E.; Bulst, W. E.; Knauer, U.; Mages, G. *Sens. Actuators, B* **1993**, *13*−*14*, 297. (b) Schierbaum, K. D.; Weiss, T.; van Velzen, E. U. T.; Engbersen, J. F. J.; Reinhoudt, D. N.; Gopel, W. *Science* **1994**, *265*, 1413. (c) Moore, L. W.; Springer, K. N.; Shi, J.-X.; Yang, X.; Swanson, B. I.; Li, D. *Adv. Mater.* **1995**, *7*, 729. (d) Dermody, D. L.; Crooks, R. M.; Kim, T. *J. Am. Chem. Soc.* **1996**, *118*, 11912. (e) Rickert, J.; Weiss, T.; G'pel, W. *Sens. Actuators, B* **1996**, *31*, 45.

(21) (a) Finklea, H. O.; Phillippi, M. A.; Lompert, E.; Grate, J. W. *Anal. Chem.* **1998**, *70*, 1368. (b) Jarrett, M. R.; Finklea, H. O. *Anal. Chem.* **1999**, *71*, 353.

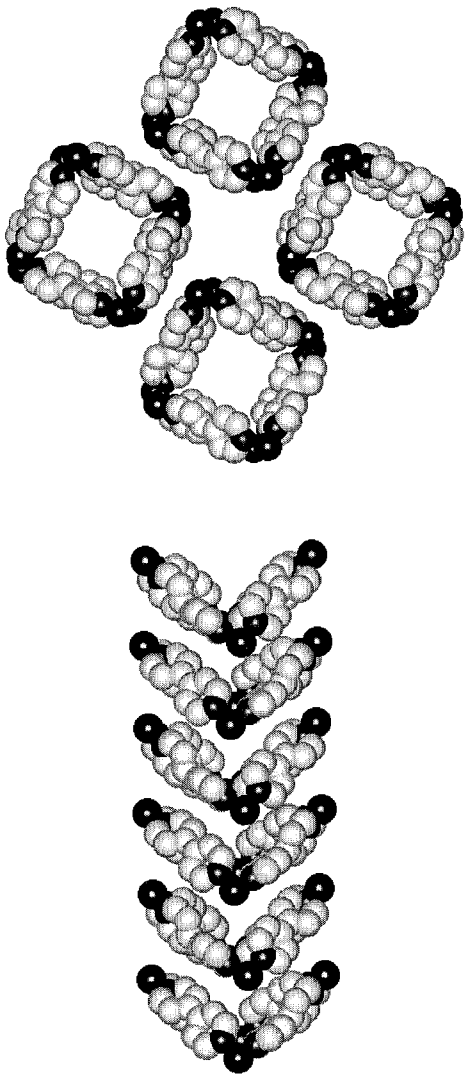

Figure 2. Top: Space-filled representation of the single-crystal X-ray structure of **2** along the *c* crystallographic axis,[13] showing the infinite channels. Bottom: Space-filled representation of the structure in the *bc* plane showing their puckered arrangement. For clarity, we have omitted the one chloro and three carbonyl ligands surrounding each metal atom (corner atom). The solvent molecules (omitted for clarity) are located along the channels, above and below the molecular squares.

Experimental Section

Materials. Neutral tetrarhenium-based molecular squares and monorhenium corners were prepared via literature methods.[4,23] Analytes were purchased from Aldrich and used as received. Solvents (reagent grade) were purchased from Fisher.

Film Preparation. Saturated solutions of the molecular squares were prepared in acetonitrile. The suspensions were sonicated, and an equal volume of chloroform was added. The mixture was filtered through a 0.1 μm polytetrafluorethylene membrane (Whatman). Thin films were deposited by spin-casting (220−650 rpm) and solvent evaporation from a chloroform/acetonitrile (1/1) solution added dropwise onto gold-coated quartz crystal resonators mounted on a photoresist spinner. Films were then placed under vacuum for 8 h, to remove excess solvent prior to the QCM studies. A new film was prepared for each study. Films of **2** were exposed to the atmosphere for approximately 2 h following vacuum treatment.

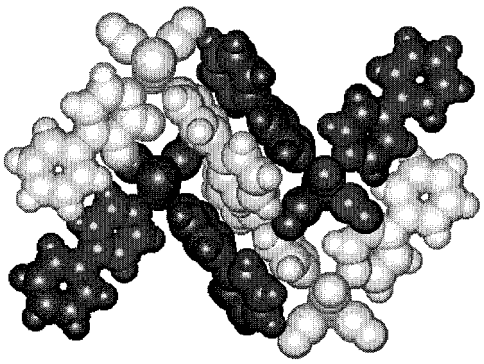

Figure 3. Space-filled representation of the single-crystal X-ray structure of **4** along the *c* crystallographic axis, illustrating the absence of channels.

QCM. QCM measurements were performed with a home-built instrument previously described.[24] Films of the molecular squares were deposited, as described above, on 5 MHz AT-cut quartz crystal resonators (ICM, Inc.). All QCM studies were performed in a sealed cell resistant to VOC adsorption. The chamber was constructed of glass with openings on both ends. Analyte introduction occurred, by injection with a 10 μL gastight syringe, through a tight-fitting screw cap with a Teflon-lined septum on one end. Analytes were chosen so that the liquid drops introduced completely evaporated within seconds. Before analyte introduction, the sealed chamber contained nitrogen. The quartz crystal was connected to the QCM instrumentation by a crystal holder machined into a Kel-F cap. Kel-F, Teflon, and glass materials were selected after significant complications related to vapor absorption were encountered with rubber-based septa and cell fittings. All of the binding constants discussed below are averages based on independent measurements with 3−6 films each.

Gas Calibration. To confirm that the QCM chamber was airtight and resistant to VOC adsorption or absorption, the vapor-phase concentrations of two aromatic guests, benzene and toluene, were confirmed by UV spectroscopy. Benzene and toluene were chosen because their standard vapor pressures, 0.119 and 0.035 atm, respectively, are from the high and low end of analytes studied. Additions of analyte of 1 μL were injected into the chamber and sampled after complete evaporation. A plot of the measured absorbance at either 254 nm (benzene) or 260 nm (toluene) versus volume of analyte added to the chamber was compared to a corresponding calibration plot calculated for complete volatilization. Experimental concentrations agreed with calculated concentrations to within 6%. Accurate analyte concentration values were necessary for the calculation of host/guest binding constants.

Crystal Structure. Single crystals of **4** were obtained via slow evaporation of a chloroform/toluene solution. Reflections were collected on an Enraf-Nonius CAD4 diffractometer using graphite-monochromated Mo K radiation. The primitive monoclinic unit cell was refined using 25 reflections ($20.14 < 2\theta < 24.04°$). Reflection data were collected up to $2\theta = 54°$ (5523 measured reflections, 5386 unique reflections). No decay correction was applied, but intensity data were corrected for absorption (analytical correction, $\mu = 54.9$ cm^{-1}, $T_{min} = 0.26$, $T_{max} = 0.66$), Lorentz, and polarization effects. The space group ($P2_1/c$) was unambiguously deduced from the systematic absences ($h0l$: $l \pm 2n$ and $0k0$: $k \pm 2n$). The structure was solved by direct methods (SIR92).[25] The non-hydrogen atoms were refined anisotropically, and hydrogen atoms were included in idealized positions but not refined. Atomic scattering factors were taken

(22) (a) Dickert, F. L.; Bäumler, U. P. A.; Stathopulos, H. *Anal. Chem.* **1997**, *69*, 1000. (b) Yang, X.; Shi, J.; Johnson, S.; Swanson, B. *Sens. Actuators, B* **1997**, *45*, 79. (c) Dickert, F. L.; Haunschild, A.; Kuschow, V.; Reif, M.; Stathopulos, H. *Anal. Chem.* **1996**, *68*, 1058. (d) Dickert, F. L.; Haunschild, A. R.; Bulst, W.-E. *Adv. Mater.* **1993**, *5*, 227. (e) Nelli, P.; Dalcanale, E.; Faglia, G.; Sberveglieri, G.; Soncini, P. *Sens. Actuators, B* **1993**, *13*, 302. Lai, C. S. I.; Moody, G. J.; Thomas, J. D. R.; Mulligan, D. C.; Stoddart, J. F.; Zarzycki, R. *J. Chem. Soc., Perkin Trans. 2* **1988**, 319.

(23) Giordano, P. J.; Wrighton, M. S. *J. Am. Chem. Soc.* **1979**, *101*, 2888.

(24) Lyon, L. A.; Hupp, J. T. *J. Phys. Chem.* **1995**, *99*, 15718.

(25) Sheldrick, G. M. In *Crystallographic Computing 3*; Sheldrick, G. M., Kruger, C., Goddard, R., Eds.; Oxford University Press: Oxford, U.K., 1985; p 175.

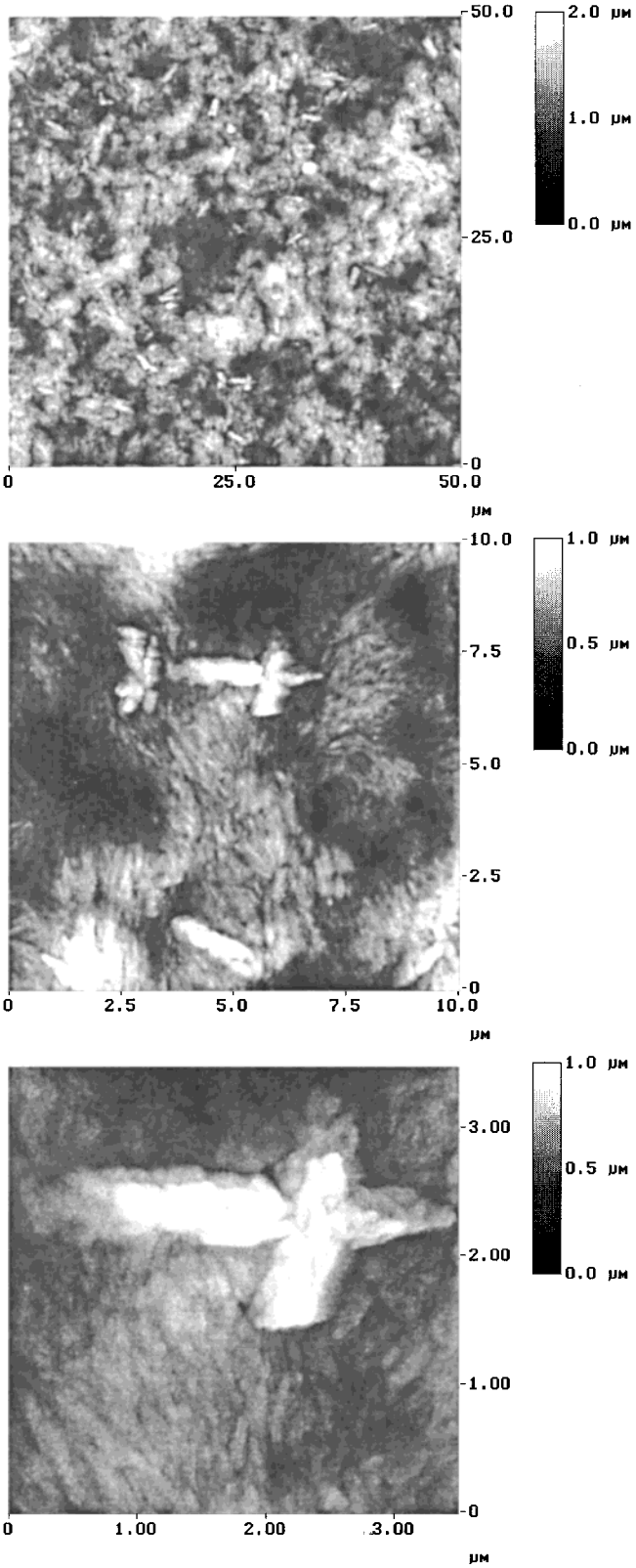

Figure 4. Representative TMAFM height images obtained in air for a thin film of **1** prepared via spin-coating/solvent evaporation on a gold-coated QCM substrate.

from the usual sources.[26] Final refinement was done by full-matrix least squares on F^2 using teXsan.[27]

Results and Discussion

Crystal Structure of 4. Structural analysis of this corner assembly shows a *fac*-octahedral geometry with dense crystals packed in a herringbone fashion. Similar corners have yielded the same geometry.[19] This packing is in contrast to the closely related square assemblies which crystallize as porous channel-containing structures. The molecular packing is shown in Figure 3 as a space-filled model positioned along the *c* crystallographic axis.

Film Characterization. Tapping mode atomic force microscopy (TMAFM) was used to characterize the resulting thin film structure and morphology. All measurements were obtained in air with a Digital Instruments Multimode Nanoscope IIIa with single etched silicon (TESP) Nanoprobe SPM tips (cantilever length 125 μm and resonance frequency 307−367 Hz, Digital Instruments). Figure 4 shows representative AFM images of a thin film of **1** on a gold-coated QCM substrate obtained via spin-casting/solvent evaporation. While continuous large-area films are produced, they are composed of an enormous number of small strandlike crystallites (~3 μm in length). Comparative TMAFM film studies on polished glass platforms (smooth platforms) yielded much more uniform collections of crystallites. The combined results suggest that the overall film morphology is largely dictated by the roughness of the underlying QCM platforms. Thus, the measured root-mean-square (rms) surface roughness for cast films of compound **1** was 220 nm, whereas the rms roughness of the gold-coated quartz resonators themselves was ca. 270 nm. Similar results were found for films of **2**. Given the high degree of roughness of the QCM platforms, AFM is not a particularly convenient methodology for determining average film thicknesses. Given these limitations, direct AFM-based comparison between the film thickness, film structure, and film porosity has not been explored. Subsequent guest uptake experiments (see below) show, however, that (a) the film *capacity* is proportional to the average film thickness, for a fixed film area, and (b) binding constants are independent of film thickness. Besides the templated roughness, the findings of significance from the AFM study are simply that the films are continuous and microcrystalline.

Average film thicknesses were determined by (1) dissolving a film in a known volume of acetonitrile or CH_2Cl_2, (2) recording an electronic absorption spectrum, and (3) using the absorbance values and the available extinction coefficients[13,28] to determine the amount of material present. All electronic absorption data were obtained on a Hewlett-Packard 8452A spectrophotometer. When the number of moles is combined with the cell parameters from the crystallographic data[4,13] of each square, an approximated film thickness could be obtained. The thicknesses here ranged from 200 to 1000 monolayers, equivalent to ~400 to ~1200 nm.

VOC Sensing: General Considerations. According to the Sauerbrey equation, mass uptake (Δm) at the quartz crystal and/or its coating is accompanied by a decrease in the crystal's fundamental frequency (f), where A_e is the electrode area:[29]

$$\Delta f = -(56.6 \text{ Hz cm}^2\ \mu\text{g}^{-1})\ \Delta m/A_e \qquad (1)$$

Figure 5 shows comparisons of the QCM response of films of **1** and **3** and a bare QCM platform to sequential

(26) *International Tables for Crystallography*; Kluwer Academic Publishers: Dordrecht, The Netherlands, 1992; Vol. C, Tables 4.2.6.8 and 6.1.1.1.

(27) *TEXSAN Single Crystal Structure Analysis*, version 1.7-1; Molecular Structure Corp.: The Woodlands, TX, 1995.

(28) (a) Wrighton, M.; Morse, D. L. *J. Am. Chem. Soc.* **1974**, *94*, 998. (b) The extinction coefficent for $Re(CO)_3Cl(4\text{-phenylpyridine})_2$ was determined in our laboratory to be 7800 M^{-1} cm^{-1} (340 nm, CH_2Cl_2).

(29) Sauerbrey, G. *Z. Phys.* **1959**, *155*, 206.

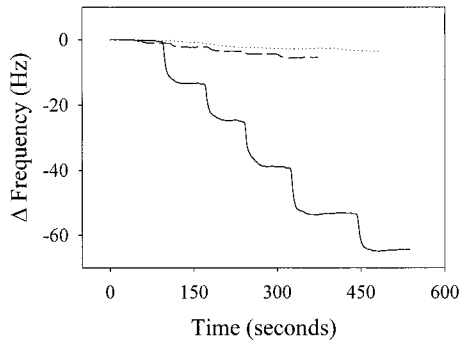

Figure 5. QCM responses of thin films of **1** (—) and **3** (– –) and a bare QCM platform (···) to sequential 1 μL benzene additions. These films contained 430 and 440 monolayers of **1** and **3,** respectively.

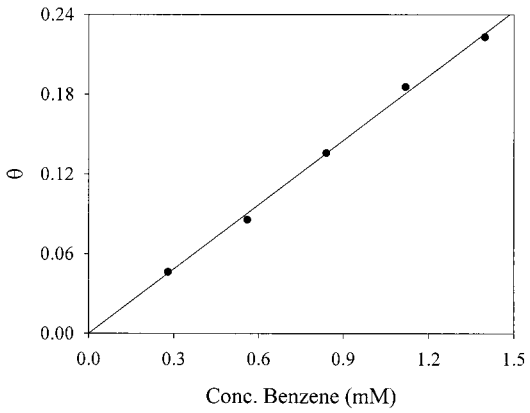

Figure 6. Fractional occupancy of the binding of benzene vapor to a crystal modified with a film of **1** fit to Henry's law adsorption isotherm (K_b = 161 M^{-1}).

increases in the benzene vapor concentration. The experiment clearly shows that VOC uptake is occurring within the thin film of **1**, whereas the film of the corner molecule **3** and the bare QCM platform are nonresponsive to the benzene vapor. Similar results are observed for the square molecule **2** (VOC uptake) and corner molecule **4** (nonresponsive).

To obtain a quantitative description of the binding interaction between various VOC guests and thin films of **1** and **2**, a simple Henry's law adsorption isotherm was invoked:

$$\Theta = K_b[\text{guest}] \qquad (2)$$

In the equation, Θ is the fractional occupancy (defined as the molar ratio of the included guest molecules to host cavity sites), K_b is the binding constant (M^{-1}), and [guest] is the vapor-phase concentration of analyte (mol/L) in the QCM chamber. In determining Θ values, we have counted intramolecular cavities but neglected interstitial cavities (cf. Figure 1). K_b was determined from plots of Θ versus [guest].[30]

Figure 6 is a fractional occupancy curve fit to Henry's law for the QCM response to benzene of the film of **1** in Figure 5. From the plot, K_b is ∼160 M^{-1}. Alternatively, the binding can be described in terms of a unitless partition coefficient, *P*, defined as the ratio of the molar concentration of the guest species in the mesoporous film to its concentration in the vapor phase.[31,32] The results in Figures 5 and 6 for **1** give *P*(benzene) = 594. The corresponding binding free energy, ΔG_b, is −16 kJ mol^{-1} at T = 298 K. If ΔG_b is calculated from K_b, assuming a standard state of 1 M, the value is −12.5 kJ mol^{-1}. Although comparisons to computationally determined binding free energies are not discussed here, we emphasize that absolute comparisons of ΔG_{calc} to experimental binding free energies are meaningful only if careful attention is paid to consistency in the choice of standard states.

Closely related to questions concerning binding strength is the issue of the analytical detection limit. If the detection limit is operationally defined as a signal present at 3 times the rms noise level (ca. 0.6 Hz in Figure 4), and if 1000 monolayers is chosen as an upper limit for the receptor film thickness (recall that signals are proportional to thickness for a mesoporous sensing layer), the binding constant from Figure 6 implies a vapor-phase benzene detection limit of 5.5 μM or 120 ppm.

Other issues of practical importance are sensor response time and reversibility. Thin films of **1** display acceptably short response times (on the order 10−50 s). Thin films of **2**, on the other hand, require as much as 30−60 min to respond fully to changes in VOC concentration. Notably, VOC-exposed films of either **1** or **2** can be readily regenerated by placing them under vacuum at ambient temperature for 10 min.

VOC Sensing: Size Selectivity. Given the fixed and uniform dimensions of the host cavities within compounds **1** and **2**, we reasoned that significant selectivity could be achieved simply on the basis of molecular size. Small guests (smaller than the available host cavities) would be susceptible to film uptake and detection, while large guests would be physically excluded and, therefore, not detected. Because of volatility limitations with larger guests and an inability, therefore, to vary the guest vapor-phase concentrations systematically, binding constants could not be obtained. Nevertheless, we found that size selectivity could be examined in the following way: Films of **1** were exposed to dioxane and to 1,4,7,10-hexaoxacyclooctadecane (18-crown-6). Dioxane is roughly the size of benzene (∼4.5 Å), whereas the mean diameter of 18-crown-6 is ∼7.5 Å, which significantly exceeds the diameter of the available cavity within square **1**. QCM studies with films of widely varying thickness showed that the absolute amount of dioxane taken up increased in proportion to the thickness or amount of the host available (ca. 5-fold thickness

(30) At higher VOC concentrations, a nonlinear QCM response was obtained, because of condensation wetting of the film and quartz. This prevented quantitative binding studies at higher fractional occupancies.

(31) Strictly speaking, only films of **2** should be described as "mesoporous" if the definition is limited to materials featuring vacancies and channels of about nanometer dimensions and larger. Using the language of zeolite chemistry, films of **1** would perhaps be better described as "microporous". Note that in this community the term describes zeolite-like materials featuring vacancies and channels of subnanometer dimension rather than micron dimension.

(32) "Mesoporosity" also typically implies a large internal surface area, where surface areas are most often determined experimentally via BET measurements using N_2 as the adsorbent. An important point, perhaps not readily appreciated, is that the QCM experiments described here are the functional equivalent of BET surface area measurements, except that the molecule of analytical interest (benzene, toluene, cyclohexane, etc.) is used in place of an arbitrary standard adsorbent. Thus, QCM-derived isotherms for porous materials can, in principle, be re-fit as BET isotherms, providing information equivalent to that provided by conventional BET measurements. For materials **1** and **2**, respectively, the minimal QCM-derived internal surface areas are 42 and 23 m^2/g, or 65 000 and 42 000 m^2/mol of molecular square. The values are conservatively calculated by using (a) the planar area of only one face of an adsorbing benzene molecule (i.e., the potential "encapsulating" nature of the host/guest interaction is ignored) and (b) the largest directly observed measures of condensation-free benzene uptake rather than the still larger values that would be derived via extrapolations of best-fit BET isotherms.

Table 1. Binding Constants for Cyclohexane and Substituted Benzenes to Films of 1 and 2

analyte	$[Re(CO)_3Cl(pz)]_4$ (**1**), M^{-1}	$[Re(CO)_3Cl(bpy)]_4$ (**2**), M^{-1}
cyclohexane	58 ± 9	17 ± 6
toluene	332 ± 26	186 ± 7
4-fluorotoluene	200 ± 42	116 ± 43
benzene	157 ± 8	103 ± 20
fluorobenzene	87 ± 8	344 ± 151

variation). Expressed another way, the fractional occupancy remained approximately constant, as expected if uptake entails host/guest complex formation. In contrast, the QCM studies of uptake of 18-crown-6 showed that the absolute amount taken up was insensitive to the film thickness or the amount of host available (ca. 5-fold thickness variation). Furthermore, the absolute amount of 18-crown-6 taken up was 1−2 orders of magnitude less (depending on film thickness) than the amount of dioxane taken up. The film-thickness observation is indicative of "uptake" of the crown via surface condensation rather than host/guest complex formation.[33] The findings are consistent, therefore, with size exclusion of 18-crown-6 by thin films of **1**.

VOC Sensing: Aromatic versus Aliphatic Guest Inclusion. In view of the aromatic nature of the bridging ligands comprising the channel walls within **1** and **2**, differences in affinity for aromatic versus aliphatic guest species might be expected. Benzene and cyclohexane were chosen for initial comparisons because they have almost identical vapor pressures and similar steric requirements. As shown in Table 1, for both squares **1** and **2** the binding constants for benzene are significantly larger than those for cyclohexane. Furthermore, the affinities of both guests for **1** are higher than those for **2**.

VOC Sensing: Guest Substituent Sensitivity. A series of substituted aromatic guests were studied with the aim of identifying additional chemical factors that might contribute favorably to binding and therefore provide an element of selectivity. With our experimental design, the guest selection was limited to volatile analytes which evaporate completely in the QCM chamber. (Unfortunately this prevented a more complete Hammett correlation study; see below.) Table 1 lists the guests and K_b's measured with thin films of **1** and **2**. Figure 7 shows that for films of **1** a correlation apparently exists between the binding constants and Hammett substituent constants (σ_p), with the more strongly electron-donating substituents (more negative σ_p values) engendering stronger complex formation. The correlation suggests that the driving force for binding is, in part, a charge-transfer interaction between the electron-rich aromatic guests and the electron-deficient pyrazine ligands.

Donor−acceptor interactions have previously been implicated in solution-phase studies of arene guest binding by highly positively charged cyclophanes (completely organic host molecules).[34] While the molecular components

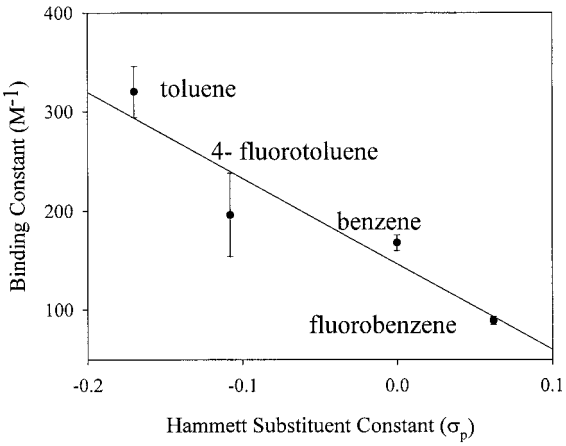

Figure 7. Correlation between the host/guest binding constants of toluene, 4-fluorotoluene, benzene, and fluorobenzene to films of **1** and the Hammett substituent constant (σ_p).[37] The σ_p value for 4-fluorotoluene used was the sum of the substituent constants for toluene and fluorobenzene.

comprising films of **1** are electrically neutral, electrochemical measurements have shown that the doubly ligated pyrazine moieties are readily reduced,[6] consistent with their characterization as electron-accepting fragments in arene−guest/host complex formation. The electrochemical studies also indicate that the bridging bipyridine ligands of compound **2** are good electron acceptors,[6] at least in an energetic sense. The lack of a convincing correlation with the Hammett constants for guest uptake by **2**, therefore, is surprising. The absence of a correlation conceivably reflects an overall poorer overlap of host/guest van der Waals surfaces here than in the complexes involving thin films of **1**. Consistent with that explanation, we find with second-generation tetrarhenium/bipyridine receptors designed to exploit guest *shape* complementarity that K_b correlates strongly with guest electron-donating capabilities.[35] Finally, for neither material do binding constants correlate with guest vapor pressure. The absence of a correlation is consistent with the conclusion that guest uptake is driven by thin-film permeation and host/guest complex formation rather than by unselective film surface condensation.

Conclusions

Mesoporous thin films based on tetrametallic molecular squares have been used to accomplish selective sensing of small molecules in the gas phase. The observed selectivity derives from host/guest size complementarity and weak chemical interactions. The component squares, which can be viewed as metal-ion-linked cyclophanes, exhibit a preference for aromatic guests over aliphatic guests and for good electron donors over poor ones. Size selectivity was also demonstrated with cyclic ethers of various size. In addition, densely packed corner analogues were shown to be blocking to VOC vapors. These preliminary sensing materials demonstrate modest sensitivity. We are currently seeking, with second-generation molecular materials, to improve on sensitivity and selectivity as well as binding strength, by exploiting shape complementarity[35] and by utilizing chemically tailorable host assemblies.[14,36]

(33) A small amount of "uptake" due to condensation is not unexpected: QCM measurements for the size-selective studies were made in an atmosphere that was saturated in crown or dioxane (with solid or liquid sample present, respectively). Experiments probing binding energies on the other interaction were performed at guest vapor pressures that were 45% or less of the saturated vapor pressure—thereby precluding condensation effects. For an instructive discussion of artifacts in SAW/QCM experiments, see: Grate, J. W.; Patrash, S. J.; Abraham, M. H.; Du, C. M. *Anal. Chem.* **1996**, *68*, 913.

(34) (a) Odell, B.; Reddington, M. V.; Stoddart, J. F.; Williams, D. J. *Angew. Chem., Int. Ed. Engl.* **1988**, *11*, 1547. (b) Bernardo, A. R.; Stoddart, J. R.; Kaifer, A. E. *J. Am. Chem. Soc.* **1992**, *114*, 10624.

(35) Benkstein, K. D.; Hupp, J. T.; Stern, C. L., submitted to *Angewante Chemie.*

(36) Bélanger, S.; Keefe, M. H.; Welch, J. L. *Coord. Chem. Rev.*, in press.

(37) McDaniel, D. H.; Brown, H. C. *J. Org. Chem.* **1958**, *23*, 420.

Acknowledgment. We thank Kurt Benkstein for providing samples of compound **1** and Dr. Keith Stevenson for machining the QCM cell and performing the AFM studies. We thank the National Science Foundation (CHE-9810483) and the National Oceanic and Atmospheric Administration for financial support.

Supporting Information Available: ORTEP view of the single crystal of **4** (with complete numbering scheme). Tables S1 and S2 contain the crystal data and selected bond length and angles. This material is available free of charge via the Internet at http://pubs.acs.org.

LA991252K